JOC The Journal of Organic Chemistry

ARTICLE

pubs.acs.org/joc

Mono- and Dicarbonyl-Bridged Tricyclic Heterocyclic Acceptors: Synthesis and Electronic Properties

Yulia A. Getmanenko,*[,†] Chad Risko,[†] Paul Tongwa,[‡] Eung-Gun Kim,[†] Hong Li,[†] Bhupinder Sandhu,[‡] Tatiana Timofeeva,[‡] Jean-Luc Brédas,[†] and Seth R. Marder*[,†]

[†]School of Chemistry & Biochemistry and Center for Organic Photonics and Electronics, Georgia Institute of Technology, 901 Atlantic Drive NW, Atlanta, Georgia 30332-0400, United States

[‡]Department of Chemistry, New Mexico Highlands University, Las Vegas, New Mexico 87701, United States

Supporting Information

ABSTRACT:

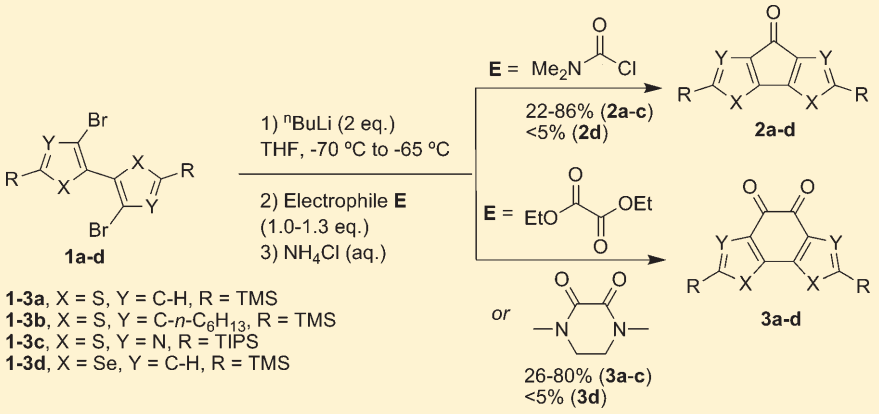

A series of trialkylsilyl-substituted 2,2′-dithiophene, 4,4′-di-*n*-hexyl-2,2′-dithiophene, 5,5′-dithiazole, and 2,2′-diselenophene with carbonyl (**2a**−**d**) and α-dicarbonyl bridges (**3a**−**d**) were prepared from readily available dihalides, using double lithiation followed by trapping with *N*,*N*-dimethylcarbamoyl chloride or diethyl oxalate (or *N*,*N*-dimethylpiperazine-2,3-dione), respectively. Cyclic voltammetry reveals that the first half-wave reduction potentials for this series of compounds span a wide range, from −1.87 to −0.97 V vs the ferrocene/ferrocenium couple at 0 V (0.1 M $^{n}Bu_4NPF_6$ in THF). A significant increase of the first half-wave reduction potential (by 0.50−0.67 V) was observed on substitution of the monocarbonyl bridge with α-dicarbonyl. Adiabatic electron affinity (AEA, gas phase) trends determined via density functional theory (DFT) calculations are in good agreement with the electrochemical reduction potentials. UV−vis absorption spectra across the series show a weak absorption band in the visible range, corresponding to the HOMO→LUMO transition within a one-electron picture, followed by a more intense, high-energy transition(s). Single-crystal X-ray structural analyses reveal molecular packing features that balance the interplay of the presence of the bulky substituents, intermolecular π-stacking interactions, and S···O intermolecular contacts, all of which affect the DFT-evaluated intermolecular electronic couplings and effective charge-carrier masses for the crystals of the tricyclic cores.

INTRODUCTION

Air-stable organic semiconductors with large electron (n-channel) mobilities are necessary for the continued development and future implementation of organic electronic devices. Over the past decade, different materials classes, e.g., perfluorinated copper phthalocyanines,[1] rylene diimides,[2,3] dicyanomethylene-substituted terthienoquinoid oligomers,[4] and dicyanomethylene derivatives of (bis)indenofluorenes,[5] have demonstrated efficient air-stable performance in n-channel organic field-effect transistors (OFET). Recently, bis-heterocyclic electron-transport materials that contain a carbonyl-bridge with either a dithiophene core (**Ia**) (electron mobility, μ_e, up to 0.08 $cm^2\ V^{-1}\ s^{-1}$)[6,7] or a dithiazole core (**Ib**) (μ_e up to 0.06 $cm^2\ V^{-1}\ s^{-1}$)[8] have been developed. Materials containing an α-dicarbonyl-bridged dithiophene, benzo[2,1-*b*:3,4-*b*′]dithiophene-4,5-dione (**II**), are still rare and only a few compounds have been reported.[9] A recent attempt to isolate 2,7-bis(thiophene-2-yl)benzo[2,1-*b*:3,4-*b*′]dithiophene-4,5-dione was reported to be unsuccessful.[10]

Ia is the most studied core among the compounds depicted in Figure 1. Synthetic approaches for **Ia** typically involve several steps,[11] starting from 3-bromothiophene and thiophene-3-carbaldehyde. **Ia** serves as a precursor for the preparation of polycyclopenta[2,1-*b*;3,4-*b*′]dithiophen-4-one derivatives,[12]

Received: December 31, 2010
Published: March 10, 2011

   dx.doi.org/10.1021/jo102502u | *J. Org. Chem.* 2011, 76, 2660–2671

4-dicyanomethylene-4*H*-cyclopenta[2,1-*b*;3,4-*b*′]dithiophene-4-one, by reaction with malononitrile,[13−17] difluoromethylene-bridged dithiophene derivatives,[18] $\Delta^{4,4'}$-dicyclopenta[2,1-*b*;3,4-*b*′]dithiophene by the reaction with Lawesson's reagent,[19] and poly-(4,4-dialkylcyclopenta[2,1-*b*;3,4-*b*′]dithiophene-2,6-diyls.[20] A short and convenient method for the introduction of the carbonyl bridge was recently reported in the synthesis of 4*H*-cyclopenta[2,1-*b*;3,4-*b*′]dithiazole-4-one (TIPS derivative of **Ib**, 99% yield),[8] when 2,2′-bis(triisopropylsilyl)-5,5′-dithiazole was lithiated with lithium diisopropylamide (LDA) followed by trapping with ethyl 1-piperidine carboxylate. A five-step synthesis of 4*H*-cyclopenta[2,1-*b*;3,4-*b*′]diselenophen-4-(1,3-dioxolane) (a derivative of **Ic**) was also reported in the literature.[21]

α-Dicarbonyl-bridged bis-heterocycles published to date are solely limited to dithiophene (**II**) derivatives to the best of our knowledge. To introduce the dicarbonyl bridge, an intramolecular benzoin condensation of 2,2′-dithiophene-3,3′-dicarbaldehyde[22] or its 5,5′-disubstituted derivatives[9] followed by air oxidation was used (23−30% yields). Condensation of benzo-[2,1-*b*:3,4-*b*′]dithiophene-4,5-dione, **II**, with diamines was reported,[23,24] as well as the preparation of 2,7-diiodobenzo[2,1-*b*:3,4-*b*′]dithiophene-4,5-dione and its attempted application in the Suzuki coupling.[10]

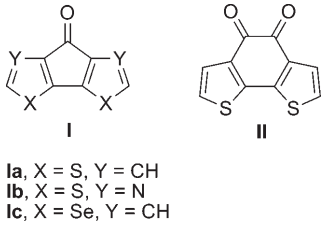

Figure 1. Structures of 4*H*-cyclopenta[2,1-*b*;3,4-*b*′]dithiophen/dithiazole/diselenophen-4-one, **I**, and benzo[2,1-*b*:3,4-*b*′]dithiophene-4,5-dione, **II**.

Recently, we have developed a convenient method[25] for the preparation of dibromo-bisarenes **1a**,**c**−**e**, Scheme 1, suitable for cyclization reactions. Here, we report a one-pot synthesis of mono- (**2a**−**d**) and α-dicarbonyl-bridged (**3a**−**d**) dithiophene, dialkyl-dithiophene, dithiazole, and diselenophene structures. The electronic properties of these tricyclic cores were studied by cyclic voltammetry, UV−vis absorption spectroscopy, and density functional theory (DFT) calculations. Three materials, 2,6-bis(triisopropylsilyl)-4*H*-cyclopenta[2,1-*b*;3,4-*b*′]dithiazole-4-one (**2c**), 2,7-bis(trimethylsilyl)benzo[2,1-*b*:3,4-*b*′]dithiophene-4,5-dione (**3a**), and 2,7-bis(triisopropylsilyl)benzo[2,1-*b*:3,4-*b*′]dithiazole-4,5-dione (**3c**), were analyzed by single-crystal X-ray structural analysis. On the basis of these crystal structures, the intermolecular electronic couplings and charge-carrier effective masses were evaluated with DFT.

RESULTS AND DISCUSSION

Synthesis. 2,6-Bis(trimethylsilyl)-4*H*-cyclopenta[2,1-*b*;3,4-*b*′]dithiophen-4-one (**2a**) was prepared in 84−86% yields from 5,5′-bis(trimethylsilyl)-3,3′-dibromo-2,2′-dithiophene (**1a**) via double lithiation with *n*-butyllithium followed by reaction with dimethylcarbamoyl chloride[26] and acidic workup with aqueous NH_4Cl as described earlier.[27] The cyclopenta[2,1-*b*;3,4-*b*′]dithiophen-4-one derivative **2b** with two *n*-hexyl chains at the 3- and 5-positions was synthesized with the intent of imparting improved solubility and processability for conjugated oligomers or polymers that may incorporate this core in the backbone. Compound **2b** was prepared by a one-pot synthesis from 3,3′,5,5′-tetrabromo-4,4′-di-*n*-hexyl-2,2′-dithiophene (**1e**) through selective lithiation at the 5- and 5′-positions with 2 equiv of *n*-butyllithium followed by reaction with 2 equiv of chlorotrimethylsilane (TMSCl) to generate 3,3′-dibromo-4,4′-di-*n*-hexyl-5,5′-bis(trimethylsilyl)-2,2′-dithiophene (**1b**), which was used in situ in the halogen−lithium exchange reaction with 2 equiv of *n*-butyllithium followed by

Scheme 1. One-Pot Synthesis of Mono- and Dicarbonyl-Bridged Tricycles 2a−d and 3a−d

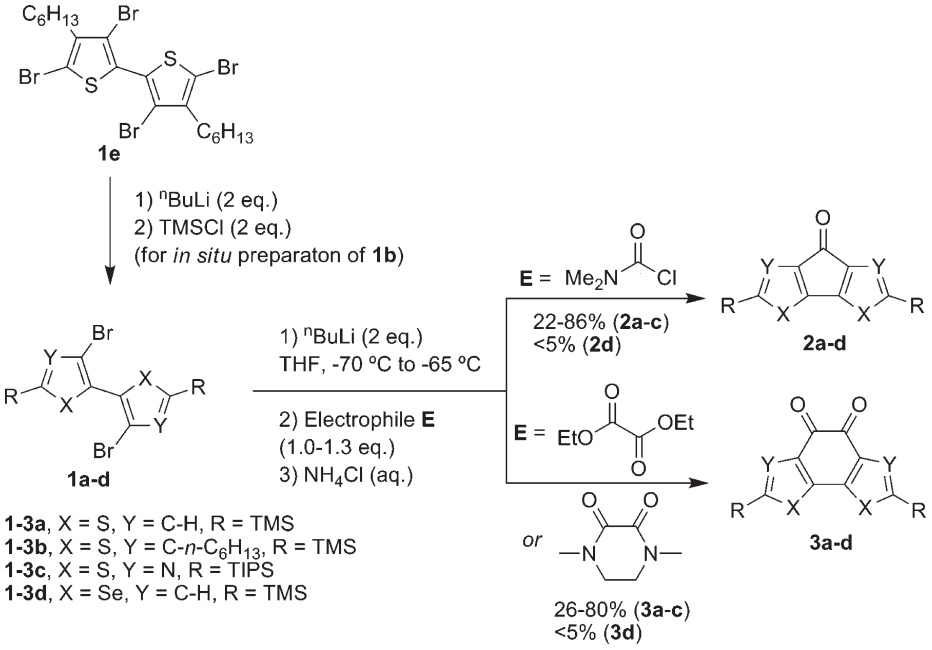

dx.doi.org/10.1021/jo102502u |*J. Org. Chem.* 2011, 76, 2660–2671

Table 1. Redox Properties of the Trialkylsilyl-Carbonyl-Containing Tricycles 2a−d and 3a−d

compd	solvent for CV[a]	$E_{1/2}^{0/1+}$, V	$E_{1/2}^{0/1-}$, V	$E_{1/2}^{1-/2-}$,[b] V	$E_{1/2}^{0/1-}$,[c] V vs SCE	AIP,[d] eV	AEA,[d] eV
2a	CH_2Cl_2	+0.96	−1.67	n/a	−1.21	7.02	−1.48
	THF	n/a	−1.74	−2.31	−1.18		
2b	CH_2Cl_2	+0.83	−1.84	n/a	−1.38	6.81	−1.41
	THF	n/a	−1.87	−2.53	−1.31		
2c	CH_2Cl_2	n/a	−1.47	−2.14	−1.01	7.51	−1.82
	THF	n/a	−1.47	−2.12	−0.91		
2d	CH_2Cl_2	+0.89	−1.61	−2.18	−1.15	6.94	−1.61
	THF	n/a	−1.67	−2.20	−1.11		
3a	CH_2Cl_2	n/a	−1.10	−1.73	−0.64	7.43	−2.08
	THF	n/a	−1.09	−1.68	−0.53		
3b	CH_2Cl_2	n/a	−1.26	−1.84	−0.80	7.20	−1.98
	THF	n/a	−1.20	−1.95	−0.64		
3c	CH_2Cl_2	n/a	−0.89	−1.58	−0.43	7.76	−2.29
	THF	n/a	−0.97	−1.73	−0.41		
3d	CH_2Cl_2	n/a	−1.00	−1.49	−0.54	7.36	−2.17
	THF	n/a	−1.04	−1.49	−0.48		

[a] CV was recorded in 0.1 M $^nBu_4NPF_6$ in specified solvent ($Cp_2Fe^{0/1+}$ internal standard at 0 V, 50 mV·s^{-1} scan rate). [b] Second reduction was partially electrochemically reversible for all compounds and $E_{1/2}^{1-/2-}$ was estimated with large error. [c] $E_{1/2}^{0/1-}$(vs SCE) = $E_{1/2}^{0/1-}$(vs Cp_2Fe) + 0.56 V (for THF); $E_{1/2}^{0/1-}$(vs SCE) = $E_{1/2}^{0/1-}$(vs Cp_2Fe) + 0.46 (for dichloromethane).[34] [d] AIP determined at the B3LYP/6-311G** level of theory, while AEA determined at the B3LYP/6-311++G** level of theory; adiabatic ionization energies determined as E(ion) − E(neutral).

reaction with *N*,*N*-dimethylcarbamoyl chloride. The reaction temperature after addition of *N*,*N*-dimethylcarbamoyl chloride must be kept below −30 to −25 °C in order to obtain 2,6-bis(trimethylsilyl)-3,5-di-*n*-hexylcyclopenta[2,1-*b*;3,4-*b*′]dithiophen-4-one (**2b**) in satisfactory yields (52−56%).[28] Lower yields (22−39%) were obtained for the 2,6-bis(triisopropylsilyl)cyclopenta[2,1-*b*;3,4-*b*′]dithiazole-4-one (**2c**) when 4,4′-dibromo-2,2′-bis(triisopropylsilyl)-5,5′-dithiazole (**1c**) was reacted with 2 equiv of *n*-butyllithium followed by cyclization using *N*,*N*-dimethylcarbamoyl chloride. Only a trace amount of desired product **2d** was obtained from 5,5′-bis(trimethylsilyl)-3,3′-dibromo-2,2′-diselenophene (**1d**) using the same reaction conditions.

Introduction of the α-dicarbonyl bridge was achieved by using either the diethyl oxalate or *N*,*N*-dimethylpiperazine-2,3-dione[29,30] electrophiles after lithiation of the dihalides **1a**−**d** with 2 equiv of *n*-butyllithium. The highest yield for 2,7-bis(trimethylsilyl)benzo[2,1-*b*:3,4-*b*′]dithiophene-4,5-dione (**3a**) was obtained when the dilithiated species generated from 5,5′-bis(trimethylsilyl)-3,3′-dibromo-2,2′-dithiophene (**1a**) was transferred via cannula into a solution of diethyl oxalate followed by transfer of the reaction mixture via cannula into an aqueous solution of NH_4Cl. Recrystallization of the crude product from ethanol produced **3a** in 54−80% yields on multigram scales (the yields for **3a** were improved from 54−61% to 76−80% when 1.3 equiv of diethyl oxalate were used instead of 1.05−1.1 equiv). *N*,*N*-Dimethylpiperazine-2,3-dione was also examined as the electrophile, and the best yield achieved for **3a** was 44% after 18 h of stirring, but this yield was not readily reproducible and low yields (<10%) were typical.[31] A lower yield of 34% in comparison with **3a** was obtained for the preparation of 2,7-bis(trimethylsilyl)-3,6-di-*n*-hexylbenzo[2,1-*b*:3,4-*b*′]dithiophene-4,5-dione (**3b**) using diethyl oxalate as the electrophile. 2,7-Bis(triisopropylsilyl)benzo[2,1-*b*:3,4-*b*′]dithiazole-4,5-dione (**3c**) was conveniently prepared in 26−40% yields using *N*,*N*-dimethylpiperazine-2,3-dione in the reaction with the dilithiated species obtained from 4,4′-dibromo-2,2′-bis(triisopropylsilyl)-5,5′-dithiazole (**1c**). Preparation of 2,7-bis(trimethylsilyl)benzo[2,1-*b*:3,4-*b*′]diselenophene-4,5-dione (**3d**) was attempted, but the desired product was isolated in a very low yield (<5%) after double lithiation of **1d** with *n*-butyllithium followed by the reaction with diethyl oxalate.

Electronic Properties. The electrochemical properties of the tricyclic aromatic cores **2a**−**d** and **3a**−**d** were examined by cyclic voltammetry (CV) in 0.1 M tetra-*n*-butylammonium hexafluorophosphate ($^nBu_4NPF_6$) in dichloromethane and THF using the ferrocene/ferrocenium couple ($Cp_2Fe^{0/1+}$) as the internal reference (see Table 1 and Figure 2; note all potentials hereafter will be reported using the ferrocene/ferrocenium couple as the reference at 0 V). By using THF as the solvent, **2a**−**d** show similar reduction behavior with each compound having two reduction waves; the second reduction is partially electrochemically reversible with $I_{red} > I_{ox}$. As expected a priori due to the inductively donating nature of the alkyl groups, introduction of *n*-hexyl groups at 3- and 5-positions of the cyclopenta[2,1-*b*;3,4-*b*′]dithiophen-4-one to form **2b** results in a shift toward more negative potential for both the first and second half-wave reduction potentials (by 0.13 and 0.22 V, respectively) vs **2a**. In contrast, substituting sulfur with selenium to form **2d** results in a less negative potential for both the first and second half-wave reduction potentials (by 0.07 and 0.11 V, respectively), hence making formation of the radical-ion more facile. The dithiazole derivative **2c**, due to the more electron-deficient nature of thiazole in comparison to thiophene,[32] exhibits the most positive first and second half-wave reduction potentials in the series with the first reduction occurring at −1.47 V.

Substituting the monocarbonyl bridge with the more electron-deficient α-dicarbonyl bridge results in a substantial increase of the first half-wave reduction potentials of **3a**−**d**, with the first half-wave reduction potentials ranging from −0.97 V for the dithiazole derivative **3c** to −1.20 V for the 3,6-di-*n*-hexyldithiophene derivative **3b** (0.1 M $^nBu_4NPF_6$ in THF). As observed for the monocarbonyl-bridged tricycles **2a** and **2d**, substitution of sulfur with selenium leads to a positive shift in both the first (by 0.05 V) and second (by 0.19 V) half-wave reduction potentials.

dx.doi.org/10.1021/jo102502u |*J. Org. Chem.* 2011, 76, 2660–2671

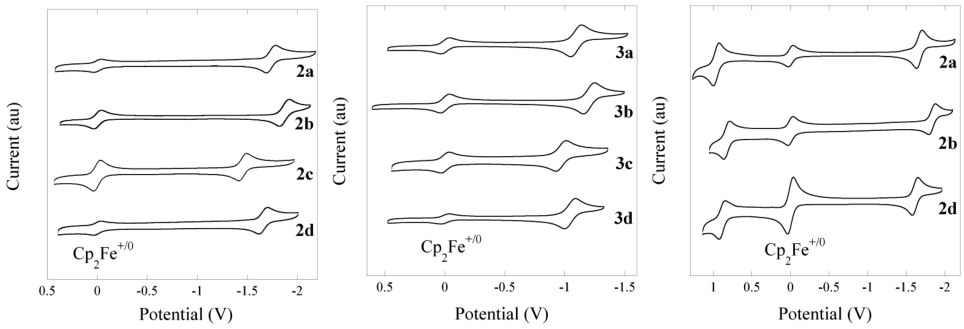

Figure 2. Normalized cyclic voltammograms (0.1 M $^{n}Bu_4NPF_6$ in THF vs $Cp_2Fe^{0/1+}$ at 0 V) of (left) monocarbonyl-bridged tricycles **2a**−**d** and (center) dicarbonyl-bridged tricycles **3a**−**d**. (right) Normalized cyclic voltammograms (0.1 M $^{n}Bu_4NPF_6$ in CH_2Cl_2 vs $Cp_2Fe^{0/1+}$ at 0 V) of monocarbonyl-bridged tricycles **2a**, **2b**, and **2d**.

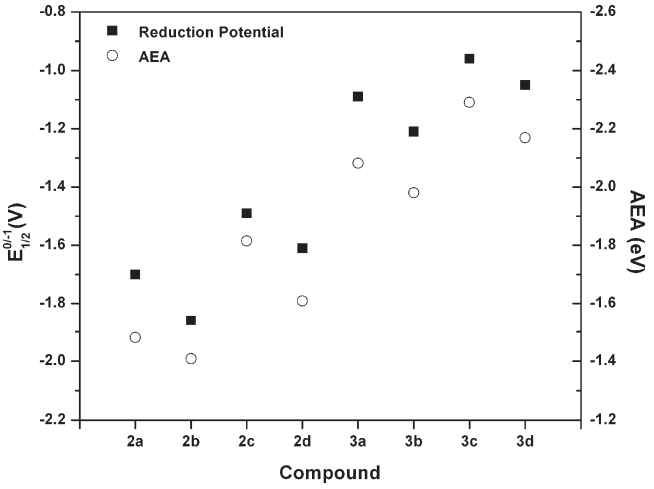

Figure 3. CV first half-wave reduction potentials (0.1 M $^{n}Bu_4NPF_6$ in THF vs $Cp_2Fe^{0/1+}$ at 0 V) versus adiabatic electron affinity (AEA) as determined at the B3LYP/6-311++G** level of theory. Note that the AEA was determined as *E*(anion) − *E*(neutral), so that a more negative (that is, exothermic) AEA indicates easier reduction.

Adiabatic electron affinity (AEA, gas phase) trends determined via density functional theory (DFT) calculations at the B3LYP/6-311++G** level are in excellent agreement with the electrochemical reduction potentials, see Table 1 and Figure 3. For both the monocarbonyl and α-dicarbonyl series, addition of the *n*-hexyl groups at 3- and 5/6-positions (**2b**/**3b**) results in a decrease of the electron affinity vs the nonalkylated (**2a**/**3a**) cores, while substituting sulfur with selenium (**2d**/**3d**) results in a slight increase of the electron affinity. Moreover, moving to the more electron-deficient dithiazole structure (**2c**/**3c**) leads to the largest increase of the adiabatic electron affinity. The lowest unoccupied molecular orbital (LUMO) energies (which can roughly be used as an estimate of the vertical electron affinity via Koopmans' theorem[33]) also reveal similar trends. Analysis of the LUMO wave functions, Figure 4, reveals, within the respective monocarbonyl and α-dicarbonyl series, that the various changes to the molecular structure produce minimal change to the overall wave function distribution. For both the mono- and α-dicarbonyl compounds, the LUMO wave function is fairly well delocalized across the entire π-conjugated system. Considerable wave function density resides within the central portions of the molecular systems, principally composed of a linear combination of the π* orbitals of

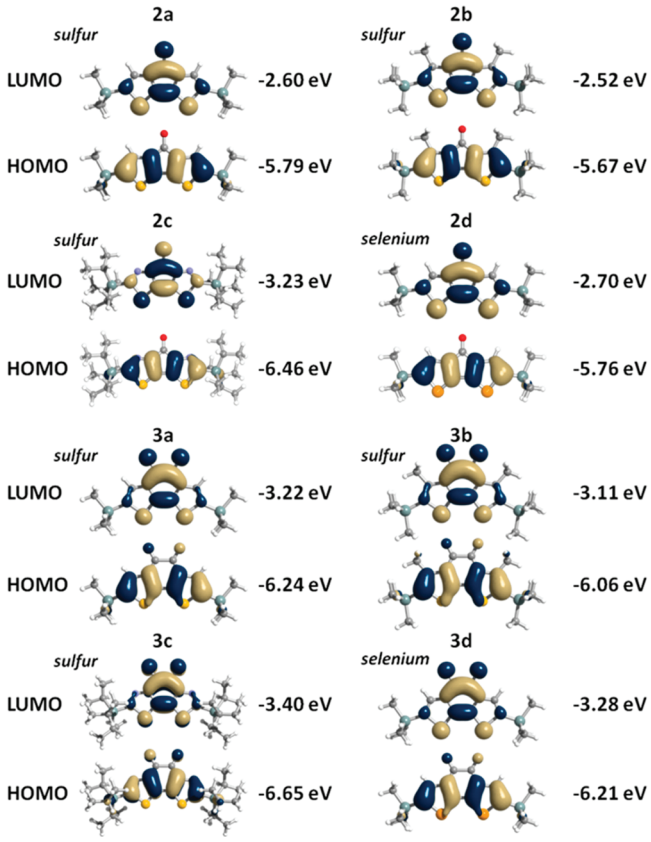

Figure 4. Frontier molecular orbital energies and wave function illustrations, as determined at the B3LYP/6-311G** level of theory.

both the *cis*-butadiene and mono/dicarbonyl moieties, respectively; substantial density also resides on the sulfur/selenium atoms. Importantly, there is sizable wave function density on the 2- and 6(7-)-positions in the mono(di)carbonyl systems. These positions can be readily substituted to extend the π-conjugation and/or increase the electron deficiency to lead to molecular systems with larger electron affinities—a parameter of importance with regard to the development of air-stable n-channel organic semiconducting materials.

The CV analysis of monocarbonyl-bridged tricycles **2a**, **2b**, and **2d** in 0.1 M $^{n}Bu_4NPF_6$ in dichloromethane (Figure 2) also shows reversible (partially in the case of **2d**) oxidation waves with the half-wave oxidation potential increasing as **2b** < **2d** < **2a**.

dx.doi.org/10.1021/jo102502u |*J. Org. Chem.* 2011, 76, 2660–2671

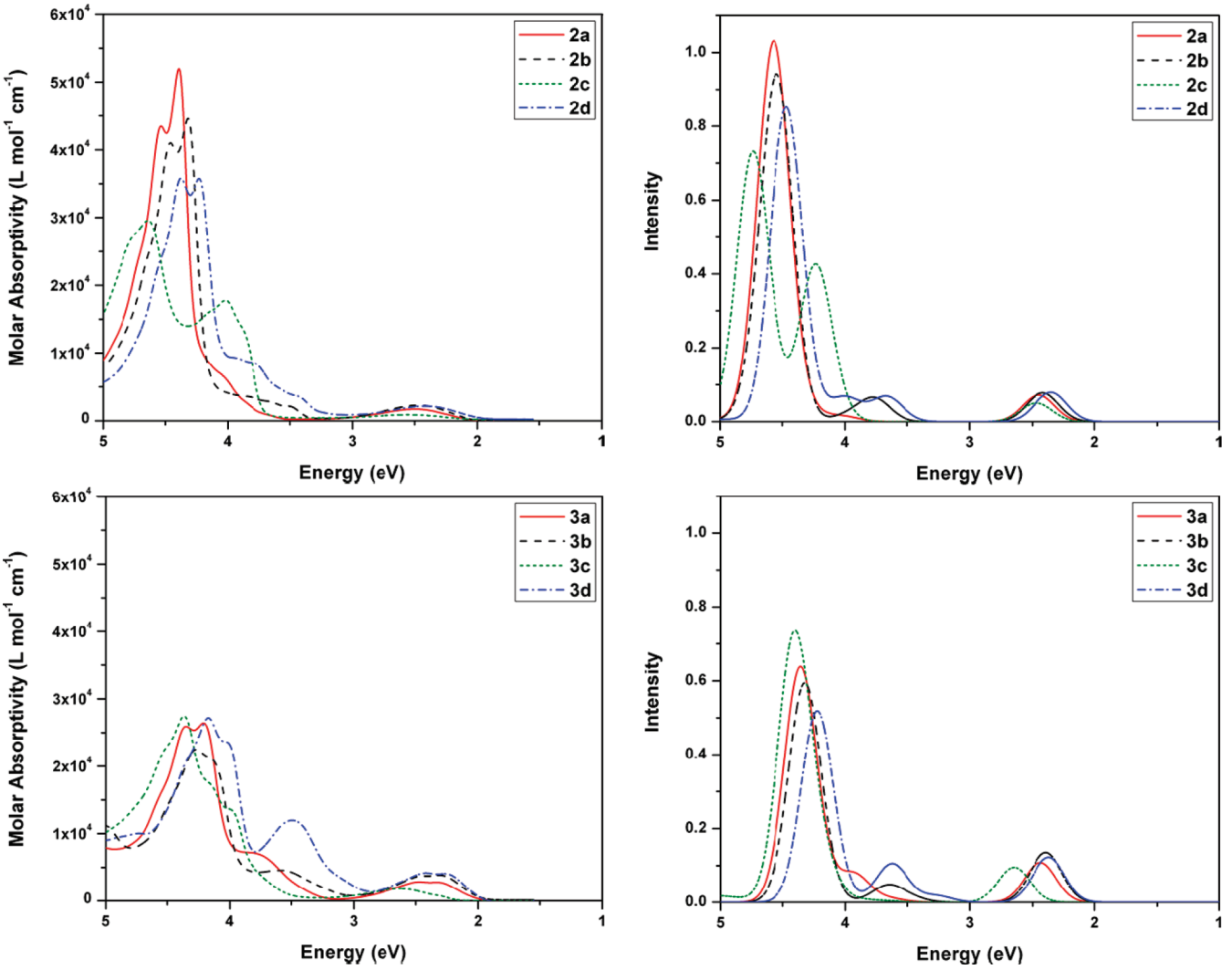

Figure 5. (left) UV−vis absorption spectra of monocarbonyl (**2a**−**d**, top) and dicarbonyl (**3a**−**d**, bottom) tricycles in dichloromethane. (right) Simulated absorption spectra for the monocarbonyl (**2a**−**d**, top) and dicarbonyl (**3a**−**d**, bottom) tricycles as determined with TDDFT at the B3LYP/6-311G** level of theory (note that the vibronic structure is not taken into account in the theoretical spectra).

However, oxidation potentials could not be measured in THF or CH_2Cl_2 for the remaining compounds. Comparison of the CV oxidation for **2a**, **2b**, and **2d** with the calculated adiabatic ionization potentials (AIPs) determined at the B3LYP/6-311G** level of theory reveals a very similar trend. Replacing the sulfur (**2a**) with selenium (**2d**) reduces the AIP (0.08 eV), while appending the inductively donating alkyl groups to the core (**2b**) stabilizes the AIP slightly more (0.21 eV). The AIP results indicate, as expected, that changing the thiophene units for the electron-deficient thiazole units significantly increases the AIP, making oxidation a much more difficult process. These trends in AIP vs substitution pattern hold for the α-dicarbonyl systems **3a**−**d** as well, with the α-dicarbonyl-bridged structures being much more difficult to oxidize in general. As with the AEA, the HOMO energies (which can be used to estimate the vertical ionization potential) trend with the AIP. The HOMO wave function distributions do not change significantly with substitution across the series, and are mainly an additive linear combination of the two thiophene (thiazole/selenophene) moiety HOMOs, with some wave function density on the oxygen atoms in the α-dicarbonyl structures.

UV−vis absorption analyses for both the mono- and dicarbonyl tricycles show a weak absorption band in the visible range followed by more intense, high-energy electronic transitions (Figure 5, Table 2). Descriptions of the excited states determined via time-dependent DFT (TDDFT) analysis at the B3LYP/6-311G** level of theory agree with the empirical results; in particular, simulated absorption profiles based on the TDDFT results match remarkably well the UV−vis data. The core π-structure for both the mono- and dicarbonyl systems possesses C_{2v} symmetry. The weak low-energy transitions are predominantly HOMO (a_2) → LUMO (b_2) electronic excitations (within the one-electron picture) of B_1 symmetry, which are transition-dipole allowed within the C_{2v} framework. For the dithiophene/diselenophene compounds, the second high-energy peak principally corresponds to a B_1 symmetry, HOMO → LUMO+1 transition. The picture is a little more complicated for the dithiazole systems (**2c**/**3c**). For **2c**, there exist two dominant high-energy transitions that each correspond to two (nearly) isoenergetic transitions comprised of a linear combination of three one-electron excitations of considerable weight. In **3c**, one

dx.doi.org/10.1021/jo102502u |*J. Org. Chem.* 2011, 76, 2660–2671

Table 2. Summary of UV−Vis Absorption Spectra and TDDFT Determination of the Optical Transitions, E_{opt}, Their Oscillator Strengths, f, and the Main Electronic Configurations Involved in the Description of the Respective Excited States

compd	λ_{max} ($\varepsilon \times 10^{-4}$ ($M^{-1}cm^{-1}$)) (CH_2Cl_2)	E_{opt} (eV)	E_{opt} (nm)	f	electronic configurations
2a	494 (0.17), 282 (5.2), 273 (4.4)	2.45	507	0.07	HOMO → LUMO (98%)
		4.57	272	0.97	HOMO → LUMO+1 (82%);
					HOMO-2 → LUMO (13%);
					HOMO → LUMO (2%)
2b	502 (0.23), 287 (4.5), 278 (4.1)	2.41	513	0.08	HOMO → LUMO (97%)
		4.54	273	0.90	HOMO → LUMO+1 (90%);
					HOMO-1 → LUMO (5%);
					HOMO → LUMO (2%)
2c	485 (0.08), 309 (1.8), 268 (3.0)	2.47	503	0.05	HOMO → LUMO (98%)
		4.22	294	0.24	HOMO-6 → LUMO (65%);
					HOMO → LUMO+1 (29%);
					HOMO-9 → LUMO (3%)
		4.26	291	0.18	HOMO → LUMO+1 (53%);
					HOMO-6 → LUMO (33%);
					HOMO-9 → LUMO (12%)
		4.74	262	0.33	HOMO-9 → LUMO (47%);
					HOMO → LUMO+3 (43%);
					HOMO → LUMO+1 (7%)
		4.76	261	0.33	HOMO → LUMO+3 (55%);
					HOMO-9 → LUMO (36%);
					HOMO → LUMO+1 (7%)
2d	512 (0.20), 293 (3.6), 283 (3.6)	2.35	528	0.08	HOMO → LUMO (98%)
		4.47	277	0.83	HOMO → LUMO+1 (91%);
					HOMO-1 → LUMO (5%)
3a	533 (0.27), 501 (0.28), 295 (2.6), 285 (2.6), 242 (0.85)	2.19	565	0.00	HOMO → LUMO+1 (97%)
		2.43	509	0.11	HOMO → LUMO (99%)
		4.36	284	0.61	HOMO → LUMO+1 (94%);
					HOMO-2 → LUMO (3%)
3b	537 (0.36), 500 (0.35), 345 (0.43), 290 (2.2)	2.21	560	0.00	HOMO-1 → LUMO (97%)
		2.39	519	0.14	HOMO → LUMO (99%)
		4.33	286	0.54	HOMO → LUMO+1 (96%)
3c	475 (0.15), 284 (2.3)	2.11	589	0.00	HOMO-1 → LUMO (97%);
					HOMO-1 → LUMO+1 (2%)
		2.65	468	0.10	HOMO → LUMO (99%)
		4.41	281	0.68	HOMO → LUMO+4 (61%);
					HOMO-9 → LUMO (35%)
3d	297 (2.7), 355 (1.2), 513 (0.41)	2.13	581	0.00	HOMO-1 → LUMO (97%);
					HOMO-1 → LUMO+1 (2%)
		2.37	524	0.12	HOMO → LUMO (99%)
		4.23	293	0.49	HOMO → LUMO+1 (92%);
		2.37	524	0.12	HOMO-1 → LUMO+1 (4%)

principal high-energy transition is present that is comprised of a linear combination of two one-electron excitations of importance.

Single-Crystal X-ray Structural Analysis. 2,6-Bis(triisopropylsilyl)cyclopenta[2,1-*b*;3,4-*b*′]dithiazole-4-one (**2c**) and 2,7-bis(triisopropylsilyl)benzo[2,1-*b*:3,4-*b*′]dithiazole-4,5-dione (**3c**) produced crystals suitable for single-crystal X-ray structural analysis by slow evaporation of dichloromethane solutions. 2,7-Bis(trimethylsilyl)benzo[2,1-*b*:3,4-*b*′]dithiophene-4,5-dione (**3a**) crystals were obtained by cooling of the hot ethanol solution.

Compound **2c** (Figure 6) crystallizes in the tetragonal $P\bar{4}2_1c$ space group with one-half molecule per asymmetric unit. The molecule resides on a 2-fold axis and is characterized by an almost planar tricyclic core, with a mean atomic deviation from the plane of 0.0102 Å. The molecules related by the 4-fold axis are held together via short C═O···S contacts [O(1)···S(1)(−0.5 − *y*, −0.5 − *x*, −0.5 + *z*) = 3.054 Å] and form slightly corrugated ribbons (Figure 7a). The dihedral angle between the tricyclic cores of the neighboring molecules in the ribbons is 16°. The ribbons are packed in a T-shape mode, as presented in Figure 7b.

Compounds **3a** and **3c** (Figure 8a,b) crystallize in the centrosymmetric orthorhombic *Pnna* and monoclinic *P*2/*n* space groups, respectively, with two halves of two crystallographically independent molecules (**A** and **B**) per asymmetric unit. The independent molecules reside on the 2-fold axes, and have similar

dx.doi.org/10.1021/jo102502u |*J. Org. Chem.* 2011, 76, 2660–2671

geometries that vary slightly with the rotation of TMS (**3a**) and TIPS (**3c**) substituents (superposition diagrams are available in the Supporting Information, Figures S10 and S13). Similar to **2c**, the central tricyclic skeleton is planar in both compounds, with mean deviations of 0.0468 and 0.0257 Å for molecules **A** and **B**, respectively, in **3a** and 0.0137 and 0.0243 Å for molecules **A** and **B**, respectively, in **3c**. The corresponding **A**/**B** dihedral angles between the planes are 8.51(1)° in **3a** (where the molecules are stacked) and 70.78(7)° in **3c** (where the molecules are in ribbons, see the Supporting Information, Figure S14).

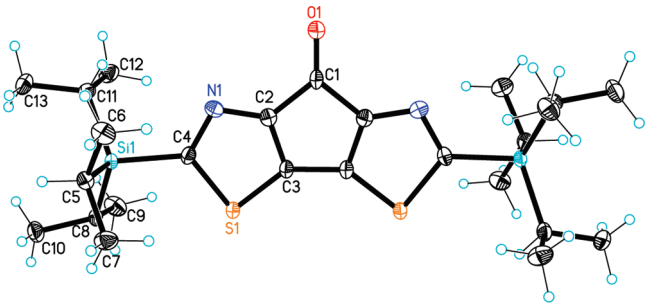

Figure 6. ORTEP drawing of **2c** (50% probability level, hydrogen atoms drawn arbitrarily small). Select bond lengths (Å): C(1)−O(1) 1.203(4), N(1)−C(2) 1.337(3), S(1)−C(3) 1.699(2), C(4)−Si(1) 1.889(2), C(2)−C(3) 1.368(3).

The crystal structures of **3a** and **3c** demonstrate differing packing motifs influenced by the size of the attached substituents. In **3a**, the alternating **A** and **B** molecules are stacked along the *b* crystallographic axis (Figure 9a), with the dihedral angle between the cores of 8.64(1)°. The shortest distances between the overlapping areas are in the range of 3.30−3.65 Å, including the short intermolecular S(1A)···S(1B) contact of 3.631 Å. The adjacent molecules in the stacks are arranged to maximize the distance between the side TMS groups (Figure 9b). For the similar structures, 4-(1,3-dithiol-2-ylidene)-4*H*-cyclopenta[2,1-*b*;3,4-*b*′]dithiophene[35] and 4-benzylidene-3,4-dihydro-1λ4-cyclopenta-[2,1-*b*:3,4-*b*′]dithiophene[36] without the side groups, the authors have previously reported the presence of only overlapping dimers with interplanar distances of 3.63 and 3.36 Å, respectively.

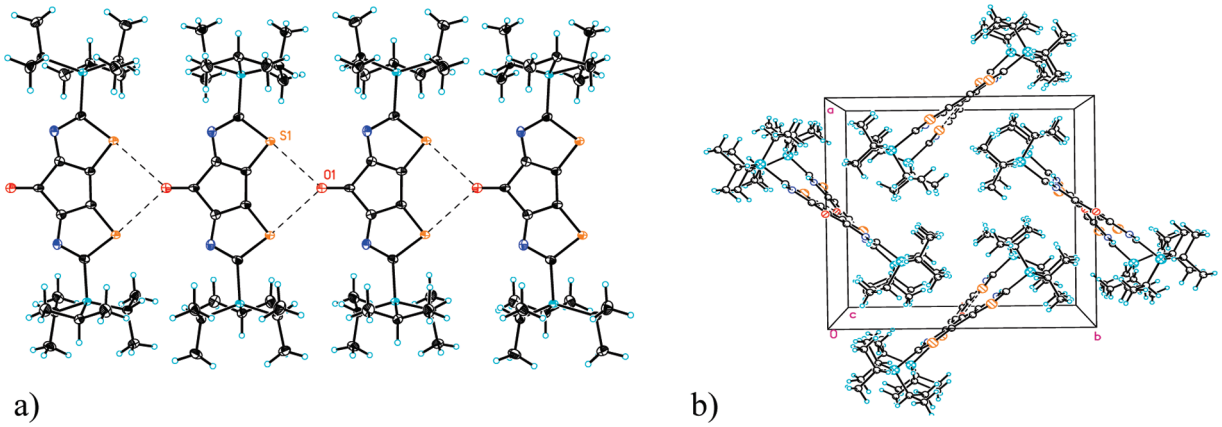

Figure 7. (a) Ribbon of **2c** molecules with short intermolecular C═O···S contacts; (b) edge-to-face arrangement of the neighboring ribbons in the crystal.

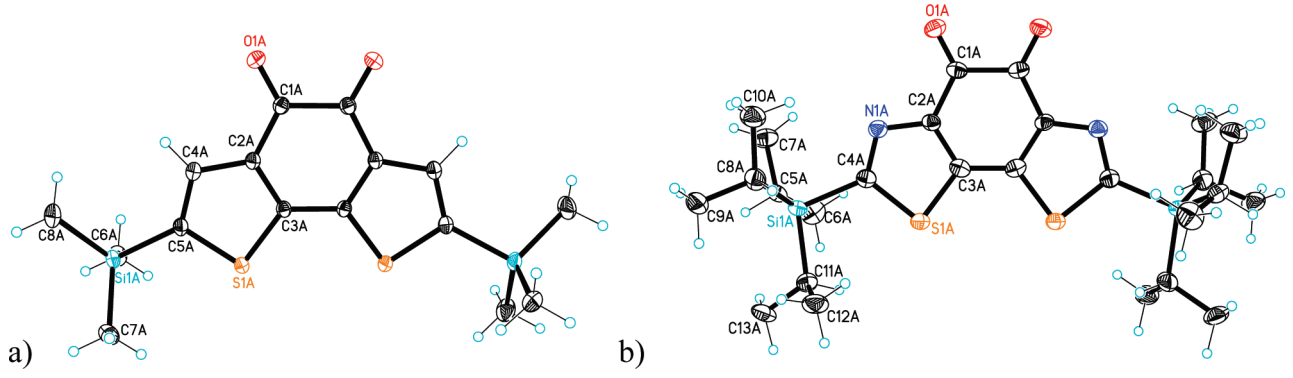

Figure 8. (a) ORTEP drawing for **3a** (50% probability level, hydrogen atoms drawn arbitrarily small). Of the two uniformly labeled molecules **A** and **B**, only molecule **A** is shown. Select bond lengths for molecule **A** in **3a** (Å): C(1A)−O(1A) 1.216(1), C(2A)−C(4A) 1.426(1), S(1A)−C(3A) 1.707(1), C(5A)−Si(1A) 1.880(1), C(2A)−C(3A) 1.385(1). Select bond lengths for molecule **B** in **3a** (Å): C(1B)−O(1B) 1.216(1), C(2B)−C(4B) 1.422(1), S(1B)−C(3B) 1.707(1), C(5B)−Si(1B) 1.879(1), C(2B)−C(3B) 1.386(1). (b) ORTEP drawing for **3c** (50% probability level, hydrogen atoms drawn arbitrarily small). Of the two uniformly labeled molecules **A** and **B**, only molecule **A** is shown. Select bond lengths for molecule **A** in **3c** (Å): C(1A)−O(1A) 1.207(6), C(2A)−N(1A) 1.398(6), S(1A)−C(3A) 1.704(5), S(1A)−C(4A) 1.770(5), C(4A)−Si(1A) 1.932(6), C(2A)−C(3A) 1.382(6). Select bond lengths for molecule **B** in **3c** (Å): C(1B)−O(1B) 1.195(5), C(2B)−N(1B) 1.376(6), S(1B)−C(3B) 1.703(4), S(1B)−C(4B) 1.740(5), C(4B)−Si(1B) 1.894(5), C(2B)−C(3B) 1.349(6).

dx.doi.org/10.1021/jo102502u |*J. Org. Chem.* 2011, 76, 2660–2671

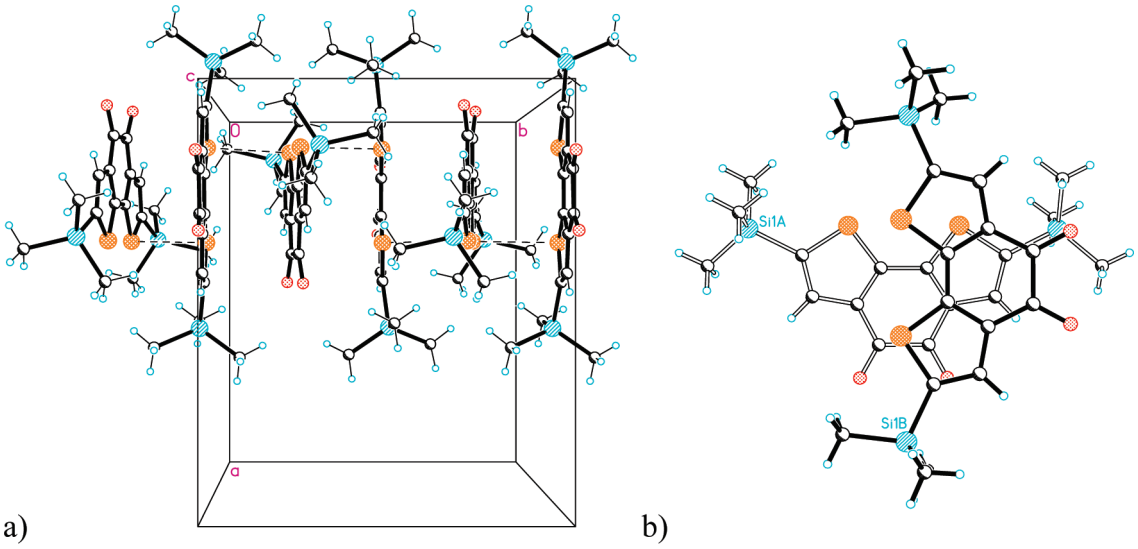

Figure 9. Stacking patterns in **3a**: (a) −A−B−A− stack in **3a** running along the crystallographic *b* axis sustained by $\pi\cdots\pi$ stacking interactions and short intermolecular S···S contacts (dashed lines); (b) overlapping area of the **A** and **B** molecules via projection on the **A** molecule (open lines).

For **3c**, the bulky TIPS substituents prevent molecular stacking, and the molecules form uniform A−A−A and B−B−B ribbons built of translational molecules arranged in an edge-to-edge mode, similar to that found in **2c**; the S···O intermolecular contacts are 3.45 and 3.48 Å, respectively, in the two ribbons. The edge-to-face ribbon packing in **3c** essentially reproduces the crystal packing of **2c** (packing diagrams are available in the Supporting Information, Figure S14). Contrary to the TMS substituents in **3a**, the more bulky TIPS groups in **2c** and **3c** prevent tight stacking interactions and, along with the short intermolecular S···O contacts, fulfill a "structure directing function" that aligns the molecules in the ribbons. A similar interplay between three effects leading to differing packing motifs was reported by Rovira and co-workers[37] for tetrathiafulvalene (TTF) derivatives: S···S contacts, π-stacking, and hydrogen bonds for the TTF derivatives vs S···O contacts, π-stacking, and TIPS/TMS substituent size for **2c**, **3a**, and **3c**.

On the basis of the crystal structures of **2c**, **3a**, and **3c**, DFT evaluations of the electronic band structures (PW91, ultrasoft pseudopotentials) and intermolecular electronic couplings (B3LYP/6-31G**, using the fragment orbital approach[38]) were carried out. For **2c**, both the top valence and bottom conduction bands are rather flat, and the smallest effective mass is found to be very high, 7.34 m_0, for electron transport along the *c* crystallographic axis. This is a consequence of the electronic couplings (transfer integrals) along the ribbon (*c* axis) being small for electrons (27 meV, LUMO−LUMO) and negligible for holes (HOMO−HOMO). For **3a**, the largest band dispersion is found to be along the *b* crystallographic axis, with an effective mass for electron transport of 2.98 m_0. The electronic coupling along the $\pi-\pi$ stacking direction (*b* axis) is determined to be quite large for electrons at 226 meV, while that for holes is only 29 meV. Interestingly, the two sets of symmetry-equivalent dimers within the *a*−*c* plane show differing strengths of electronic coupling for electrons (54 meV vs 9 meV); electron transport along this direction is expected to remain small. These results suggest that electron transport in **3a** should principally be one-dimensional along the molecular stacking direction. The monoclinic **3c** structure shows similar band dispersions for both the lowest conduction band and the highest valence band along the *b* crystallographic axis, with both bands being composed of two degenerate bands. Differing from **3a**, the conduction band minimum and the valence band maximum for **3c** are found to be at the Y-point and Γ-point, respectively, indicating an indirect band gap for **3c** (see the Supporting Information). The effective masses for both electron and hole transport are evaluated to be 4.59 m_0 and 5.28 m_0, respectively. As with **2c**, the electronic coupling along the ribbon (*b* axis) pathway is small for electrons (24 meV) and negligible for holes. Overall, given these band-structure characteristics, the charge-carrier mobilities in these crystals are not expected to reach large values.

CONCLUSIONS

In summary, we have described a convenient and, in some cases, efficient synthetic route toward dithiophene-, dialkyldithiophene-, dithiazole-, and diselenophene-based tricycles with mono- and α-dicarbonyl bridges. There is excellent agreement in the description of the electronic and optical properties via CV, UV−vis, and DFT analyses. The single-crystal X-ray structural analyses show interesting molecular packing features that balance the interplay of the presence of the bulky substituents, intermolecular π-stacking interactions, and S···O intermolecular contacts. The substantial increases in electron affinity for the α-dicarbonyl-bridged tricycles in comparison with monocarbonyl-bridged systems make these cores attractive for incorporation into electron-transporting organic semiconductors with potentially air-stable OFET operation.

EXPERIMENTAL SECTION

Computational Methodology. Quantum-chemical calculations of the neutral, radical-anion, and radical-cation states of **2a**−**d** and **3a**−**d** were performed at the density functional theory (DFT) level using the hybrid, generalized gradient approximation (GGA) functional B3LYP[39−41] and a 6-311G** basis set. Further analyses of the neutral and radical-anion states were carried out using the 6-311++G** basis set to more accurately determine the adiabatic electron affinities. The *n*-hexyl chains in **2b**/**3b** were truncated to methyl groups to reduce the

computational requirements. Time-dependent DFT (TDDFT) calculations were performed to assess the excited-state vertical transition energies, oscillator strengths, and electronic configurations. Absorption spectra were simulated through convolution of the vertical transition energies and oscillator strengths with Gaussian functions characterized by a full width at half-maximum (fwhm) of 0.3 eV. All single-molecule calculations were performed with Gaussian 09 (Revision A.02),[42] and molecular orbital density plots were generated with ArgusLab 4.0.1.[43] Band structure calculations at the DFT level were carried out by using the Vienna Ab Initio Simulation Package (VASP)[44,45] with ultrasoft pseudopotentials. The GGA functional of Perdew and Wang (PW91)[46] was used as the exchange and correlation potential. A plane wave cutoff of 400 eV and a total energy convergence of 10^{-6} eV for the self-consistent iteration were applied for the calculations.

Solvents. Tetrahydrofuran (THF) was freshly distilled from benzophenone ketyl; anhydrous dimethylformamide (DMF) and diethyl ether were used as received. ^{1}H and ^{13}C{^{1}H} and DEPT-135 NMR spectra were acquired in $CDCl_3$ (peaks in ^{1}H NMR were referenced to residual $CHCl_3$ signal at δ 7.27 ppm or tetramethylsilane at δ 0.00 ppm). Diethyl oxalate was dried over Na_2CO_3, then distilled under nitrogen and stored over molecular sieves. *N*,*N*-Dimethylpiperazine-2,3-dione was prepared according to the literature procedure.[30] Dibromobisarenes **1a**,**c**−**d** and 3,3′,5,5′-tetrabromo-4,4′-di-*n*-hexyl-2,2′-dithiophene (**1e**) were prepared by using the literature method.[25] 4,4′-Dibromo-2,2′-bis(triisopropylsilyl)-5,5′-dithiazole (**1c**) was also prepared by using the optimized procedure (vide infra). UV−vis absorption spectra were recorded in 1 cm cells. All materials **2a**−**d** and **3a**−**d** were purified, characterized, and stored in air.

Cyclic voltammetry was carried out under nitrogen on dry deoxygenated dichloromethane or THF solutions ca. 10^{-4} M of analyte and 0.1 M solution of tetra-*n*-butylammonium hexafluorophosphate, using a potentiostat, a glassy carbon working electrode, a platinum auxiliary electrode, and, as a pseudoreference electrode, a silver wire anodized in 1 M aqueous potassium chloride. Potentials were referenced to ferrocenium/ferrocene ($Cp_2Fe^{0/1+}$) as an internal standard at 0 V. Cyclic voltammograms were recorded at scan rates of 50 mV·s^{-1}.

The X-ray diffraction data for compounds **2c**, **3a**, and **3c** were collected at 100 K, using Mo Kα radiation (λ= 0.71073 Å) at 100 K. Absorption corrections were applied by using the semiempirical method of the SADABS program,[47] except for the case of the twinned crystal of compound **3a** and **3c**, for which TWINABS[48] was used. The structures were solved by direct methods and refined by full matrix least-squares on F^2 in the anisotropic approximation for non-hydrogen atoms. Data reduction and further calculations were performed by using the Bruker SAINT[49] and SHELXTL NT[50] program packages. All hydrogen atoms were placed in idealized positions and refined with constrained C−H distances and U_{iso} (H) values set to 1.2Ueq or 1.5Ueq (for methyl group) of the attached C atom. Selected refinement data and structure parameters are shown in the Supporting Information (Table S1).

2,6-Bis(trimethylsilyl)cyclopenta[2,1-*b*;3,4-*b*′]dithiophen-4-one (2a). The title compound was prepared from 3,3′-dibromo-5,5′-bis(trimethylsilanyl)-2,2′-dithiophene (**1a**) by using the literature procedure.[27]

2,6-Bis(trimethylsilyl)-3,5-di-*n*-hexylcyclopenta[2,1-*b*;3,4-*b*′]dithiophen-4-one (2b). 3,3′,5,5′-Tetrabromo-4,4′-di-*n*-hexyl-2,2′-dithiophene (**1e**) (23.0 mmol, 14.95 g) was dissolved in 200 mL of anhydrous tetrahydrofuran (THF), the solution was cooled in an acetone/dry ice bath, and *n*-butyllithium (2.5 M in hexanes, 46.0 mmol, 18.4 mL) was added dropwise (−70 to −65 °C). During the addition of *n*-butyllithium the light yellowish reaction mixture became darker in color (yellow-orange), but when ∼1.5 mL of *n*-butyllithium was still in the syringe, the mixture became lighter yellow. The reaction mixture was stirred for 0.5 h and chlorotrimethylsilane (46.0 mmol, 5.00 g) was added dropwise (exothermic reaction), then the solution was stirred for 20 min and analyzed by GC/MS. Clean formation of 3,3′-dibromo-4,4′-di-*n*-hexyl-5,5′-bis(trimethylsilyl)-2,2′-dithiophene was confirmed and *n*-butyllithium (2.5 M in hexanes, 46.0 mmol, 18.4 mL) was added dropwise (−70 to −68 °C internal temperature). The reaction mixture was analyzed by GC/MS after 5 min of stirring and clean lithiation was confirmed. *N*,*N*-Dimethylcarbamoyl chloride (23.0 mmol, 2.47 g) in 10 mL of anhydrous THF was added dropwise and the mixture became darker yellow. The reaction flask was partially removed from the cooling bath and the mixture was warmed to −40 to −30 °C. After 40 min of stirring the mixture was analyzed by TLC (hexanes:ethyl acetate (20:1)) and a spot subsequently indentified as the product was detected as a major material. The mixture was stirred for 1.5 h, treated with aqueous NH_4Cl (12 g in 50 mL of water) (ca. −30 °C initial internal temperature), and warmed to room temperature, then the dark red organic phase was separated. The aqueous phase was extracted with hexanes and the combined organic phases were dried over $MgSO_4$. The solvent was removed by rotary evaporation and the crude product was obtained as a thick red oil. This material was purified by column chromatography (200 mL of silica gel, hexanes as eluant). Fractions with a pure material were combined, the solvent was removed, and the product was dried under vacuum (3.72 g). The fractions with slightly contaminated material were combined separately and further purified by column chromatography to give dark red oil, which solidified on standing (2.73 g). The yield of the pure material was 55.6% (6.45 g). ^{1}H NMR ($CDCl_3$, 400 MHz) δ 2.66 (m, 4H), 1.55 (m, 4H), 1.40−1.25 (m, 12H), 0.87 (t, J = 6.8 Hz, 6H), 0.31 (s, 18H); ^{13}C{^{1}H} NMR ($CDCl_3$, 100 MHz) δ 184.5, 153.0, 147.4, 143.5, 137.1, 31.7, 31.1, 29.7, 29.3, 22.7, 14.1, 0.4; HRMS (EI) calcd for $C_{27}H_{44}OS_2Si_2$ 504.2370, found 504.2362. Anal. Calcd for $C_{27}H_{44}OS_2Si_2$: C, 64.22; H, 8.78. Found: C, 64.22; H, 8.94.

2,6-Bis(triisopropylsilyl)cyclopenta[2,1-*b*;3,4-*b*′]dithiazole-4-one (2c)

2-(Triisopropylsilyl)thiazole: 2-Bromothiazole (0.12 mol, 19.68 g) was dissolved in 180 mL of anhydrous diethyl ether and the colorless solution was cooled in an acetone/dry ice bath under nitrogen atmosphere. Triisopropylsilyl chloride (TIPSCl) (0.12 mol, 23.14 g) was added to the colorless solution followed by a dropwise addition of *n*-butyllithium (2.45 M in hexanes, 0.12 mol, 49.0 mL (**caution**: added in several portions with volume less than 20 mL)) (exotherm). Yellow-orange solution was stirred for 0.5 h and anhydrous THF (20 mL) was added ("smoke" on the contact of the solvent and reaction mixture was observed). Within a few minutes formation of a heavy precipitate was observed. Additional THF (20 mL + 40 mL + 40 mL + 20 mL) was added in portions and the beginning of the formation of 2-(triisopropylsilyl)thiazole was confirmed by GC/MS analysis (unreacted triisopropylsilyl chloride was detected as well). The reaction mixture was allowed to warm to room temperature overnight and then treated with water. The organic phase was removed and the aqueous phase was extracted with hexanes several times. The combined organic phases were dried over $MgSO_4$, the drying agent was filtered off, and the solvents were removed by rotary evaporation. The crude product was obtained as a brown oil (32.29 g). This material was purified by Kugelrohr distillation and the product was obtained as a yellowish oil (100−120 °C/1.0−1.2 mmHg) (25.35 g, 87.5% yield). ^{1}H NMR (400 MHz, $CDCl_3$) δ 8.17 (d, J = 3.0 Hz, 1H), 7.54 (d, J = 2.6 Hz, 1H), 1.46 (septet, J = 7.5 Hz, 3H), 1.14 (d, J = 7.5 Hz, 18H); ^{13}C{^{1}H} NMR (100 MHz, $CDCl_3$) δ 169.7 (quaternary C), 145.4 (CH), 121.0 (CH), 18.4 (CH), 11.6 (CH_3). (This analysis is in agreement with the literature data.[51])

Note: It is important to use diethyl ether for the lithiation of 2-bromothiazole to avoid decomposition of 2-lithiothiazole (which was often observed in THF when an acetone/dry ice bath was used as a coolant). A very sluggish reaction of 2-lithiothiazole with TIPSCl in

diethyl ether was observed (even after warm up to room temperature), and addition of THF after the lithiation step is required for successful preparation of 2-(triisopropylsilyl)thiazole.

4,4′-Dibromo-2,2′-bis(triisopropylsilyl)-5,5′-dithiazole (1c). 2-(Triisopropylsilyl)thiazole (20.0 mmol, 4.83 g) was dissolved in 100 mL of anhydrous THF under nitrogen atmosphere and the solution was cooled in an acetone/dry ice bath. *n*-Butyllithium (2.45 M in hexanes, 20.0 mmol, 8.2 mL) was added dropwise to a yellowish solution. The mixture became darker yellow (exotherm) and after a few minutes of stirring precipitate formed. After 15 min of stirring bromine (1 equiv, 20.0 mmol, 3.20 g) was added dropwise to a thick suspension and yellowish solution formed after stirring. GC/MS analysis showed a clean formation of 2-(triisopropylsilyl)-5-bromothiazole, and LDA (1.2 M in hexanes:THF, 1.1 equiv, 22.0 mmol, 18.3 mL) was added dropwise. The reaction mixture was stirred for 10 min and analyzed by TLC (several drops of the reaction mixture were treated with water and organic matter was extracted with hexanes and analyzed). A new less polar spot, which corresponds to a product of the base-catalyzed halogen dance reaction, 2-(triisopropylsilyl)-4-bromothiazole, was detected and anhydrous $CuCl_2$ (1.1 equiv, 22.0 mmol, 2.96 g) was added to a yellow-orange solution. The mixture became yellow-brown (in some cases dark purple or blue color was observed) and after 2 h of stirring it was allowed to warm to room temperature. GC/MS analysis showed a clean formation of the desired product (molecular ion of 638). The greenish reaction mixture was diluted with hexanes (~100 mL) and filtered through silica gel plug, using hexanes as eluant. The solvents were removed from the yellowish solution and the crude product was obtained as a yellow-orange solid (7.1 g, contains some solvent). This crude product was recrystallized from ethanol (~170 mL) and beige plates were obtained after vacuum filtration (4.58 g, 71.7%). The solvent was removed from the mother liquor and the residue was recrystallized from ~10 mL of ethanol. Additional product was obtained (0.58 g, 9.1%). ^{1}H NMR and $^{13}C\{^1H\}$ NMR analyses are in agreement with the literature data.[25]

4,4′-Dibromo-2,2′-bis(triisopropylsilyl)-5,5′-dithiazole (**1c**) (2.0 mmol, 1.277 g) was dissolved in 80 mL of anhydrous THF under nitrogen atmosphere, then the resulting colorless solution was cooled in acetone/dry ice bath and *n*-butyllithium (2.5 M in hexanes, 4.0 mmol, 1.6 mL) was added dropwise. The yellow solution was stirred for 20 min, and *N*,*N*-dimethylcarbamoyl chloride (2.0 mmol, 0.215 g) in 1 mL of anhydrous THF was added dropwise. The reaction flask was partially removed from the cooling bath, then the yellow-orange mixture was stirred for 1 h and treated with aqueous NH_4Cl. The red organic phase was removed, the aqueous phase was extracted with hexanes, and combined organic phases were dried over $MgSO_4$. The solvents were removed by rotary evaporation and the red residue was purified by column chromatography (150 mL of silica gel, CH_2Cl_2 as eluant). The solvent was removed from combined fractions and red solid was obtained (0.392 g, 38.8% yield). ^{1}H NMR ($CDCl_3$, 400 MHz) δ 1.46 (septet, J = 7.4 Hz, 6H), 1.14 (d, J = 7.5 Hz, 36H); $^{13}C\{^1H\}$ NMR ($CDCl_3$, 100 MHz) δ 179.0, 174.0, 158.2, 145.3, 18.4, 11.6; HRMS (EI) calcd for $C_{25}H_{42}N_2OS_2Si_2$ 506.2277, found 506.2239. Anal. Calcd for $C_{25}H_{42}N_2OS_2Si_2$: C, 59.23; H, 8.35; N, 5.53. Found: C, 59.43; H, 8.44; N, 5.55.

2,6-Bis(trimethylsilyl)cyclopenta[2,1-*b*;3,4-*b*′]diselenophene-4-one (2d). 5,5′-Bis(trimethylsilyl)-3,3′-dibromo-2,2′-diselenophene (**1d**) (1.2 mmol, 0.675 g) was dissolved in anhydrous THF (40 mL) under nitrogen atmosphere and the resulting yellow solution was cooled in an acetone/dry ice bath. *n*-Butyllithium (1.6 M in hexanes, 2.4 mmol, 1.5 mL) was added dropwise and the yellow mixture turned orange, then dark orange, and then brown. A solution of dimethylcarbamoyl chloride in THF (0.40 g in 3 mL was prepared, 1 mL was used, 1.2 mmol, 0.13 g) was added after 10 min of stirring and the dark red-orange mixture was partially removed from the cooling bath. The reaction mixture was slowly warmed to ~0 °C over 1.5 h and an aqueous solution of NH_4Cl was added. The red-brown organic phase was removed, the aqueous phase was extracted with hexanes, and combined organic phases were dried over $MgSO_4$. The solvents were removed by rotary evaporation and the crude product obtained as a dark reddish oil was purified by column chromatography (30 mL of silica gel, hexanes:CH_2Cl_2 (4:1) as eluant). The solvents were removed from combined fractions and a few milligrams of the product were obtained as a dark red solid. ^{1}H NMR ($CDCl_3$, 400 MHz) δ 7.34 (s with two satellites, 2H), 0.32 (s, 18H); $^{13}C\{^1H\}$ NMR ($CDCl_3$, 100 MHz) δ 184.9, 161.2, 153.2, 145.7, 129.2, 0.2; HRMS (EI) calcd for $C_{15}H_{20}OSe_2Si_2$ 431.9383, found 431.9390. Elemental analysis was not obtained due to the very limited amount of material.

2,7-Bis(trimethylsilyl)benzo[2,1-*b*:3,4-*b*′]dithiophene-4,5-dione[31] (3a). 3,3′-Dibromo-5,5′-bis(trimethylsilyl)-2,2′-dithiophene (**1a**) (60.0 mmol, 28.11 g) was dissolved in anhydrous THF (240 mL), the solution was cooled in an acetone/dry ice bath, and *n*-butyllithium (2.87 M in hexanes, 2 equiv, 120.0 mmol, 41.8 mL (**caution**: added in several portions with volume less than 20 mL)) was added dropwise. The yellow-orange solution was stirred for 0.5 h and then transferred via cannula into a solution of diethyl oxalate (1.3 equiv, 78.0 mmol, 11.40 g) in 200 mL of anhydrous THF (cooled in an acetone/dry ice bath). After completion of the addition of the dilithiated species to the diethyl oxalate, the orange-reddish mixture was stirred for 45 min and transferred via cannula into a solution of aqueous NH_4Cl. The dark red organic phase was separated, the aqueous phase was extracted with hexanes, and the combined organic phases were dried over $MgSO_4$. The solvents were removed by rotary evaporation and the crude product was heated to reflux with ~500 mL of ethanol and cooled to room temperature, then the dark-red needles were separated by vacuum filtration (16.3 g, 76.7% yield). The mother liquor was subjected to rotary evaporation and the residue was recrystallized from ethanol to give an additional amount of product (0.7 g, total yield 17.0 g, 79.9%). ^{1}H NMR ($CDCl_3$, 400 MHz) δ 7.60 (s, 2H), 0.36 (s, 18H, $6CH_3$); $^{13}C\{^1H\}$ NMR ($CDCl_3$, 100 MHz) δ 175.2 (quaternary C), 148.3 (quaternary C), 142.5 (quaternary C), 135.8 (quaternary C), 134.4 (CH), −0.44 (CH_3); HRMS (EI) calcd for $C_{16}H_{20}O_2S_2Si_2$ 364.0443, found 364.0469. Anal. Calcd for $C_{16}H_{20}O_2S_2Si_2$: C, 52.70; H, 5.53. Found: C, 52.70; H, 5.36.

2,7-Bis(trimethylsilyl)-3,6-di-*n*-hexylbenzo[2,1-*b*:3,4-*b*′]dithiophene-4,5-dione (3b). 3,3′,5,5′-Tetrabromo-4,4′-di-*n*-hexyl-2,2′-dithiophene (**1e**) (3.08 mmol, 2.00 g) was dissolved in 60 mL of anhydrous THF under nitrogen atmosphere, the solution was cooled in an acetone/dry ice bath, and *n*-butyllithium (2.5 M in hexanes, 6.15 mmol, 2.5 mL) was added dropwise to the yellowish solution. The reaction mixture was stirred for 15 min and chlorotrimethylsilane (6.15 mmol, 0.67 g) was added dropwise. The mixture was stirred for 15 min and *n*-butyllithium (2.5 M in hexanes, 6.15 mmol, 2.5 mL) was added dropwise. The reaction mixture was stirred for 0.5 h and the yellow solution was transferred via cannula to a solution of diethyl oxalate (4.24 mmol, 0.62 g) in 60 mL of THF cooled in an acetone/dry ice bath. The dark yellow-brown reaction mixture was stirred for 0.5 h and transferred via cannula to an aqueous solution of NH_4Cl (13 g in 50 mL of water). The dark red organic phase was separated, the organic phase was dried over $MgSO_4$, the drying agent was filtered off, and the solvents were removed by rotary evaporation to give the crude product as a red thick oil. This material was purified by column chromatography (250 mL of silica gel, hexanes:CH_2Cl_2 (3:2) to pack the column, hexanes to elute byproducts, and then hexanes:CH_2Cl_2 (3:2) to elute the product). Solvents were removed from combined fractions (red) to give a dark red oil that was dried under vacuum (the oil solidified on standing, 0.56 g, 34.1%). ^{1}H NMR ($CDCl_3$, 400 MHz) δ 2.89 (poorly resolved t, 4H), 1.47 (m, 8H), 1.33 (m, 8H), 0.90 (poorly resolved t, 6H), 0.39 (s, 18H); $^{13}C\{^1H\}$ NMR ($CDCl_3$, 100 MHz) δ 175.8 (quaternary C(O), 154.0

(quaternary C), 149.1 (quaternary C), 135.0 (quaternary C), 133.3 (quaternary C), 31.6 (CH_2), 30.9 (CH_2), 30.8 (CH_2), 29.8 (CH_2), 22.7 (CH_2), 14.1 (CH_3), 0.2 (CH_3) (the assignment of the carbon signals was made based on the DEPT experiment); HRMS (EI) calcd for $C_{28}H_{44}O_2S_2Si_2$ 532.2321, found 532.2325. Anal. Calcd for $C_{28}H_{44}O_2S_2Si_2$: C, 63.10; H, 8.32. Found: C, 62.89; H, 8.40.

2,7-Bis(triisopropylsilyl)benzo[2,1-*b*:3,4-*b*′]dithiazole-4,5-dione (3c). 4,4′-Dibromo-2,2′-bis(triisopropylsilyl)-5,5′-dithiazole (**1c**) (2.0 mmol, 1.277 g) was dissolved in 40 mL of anhydrous THF under nitrogen atmosphere and the colorless solution was cooled in an acetone/dry ice bath. *n*-Butyllithium (2.45 M in hexanes, 4.0 mmol, 1.6 mL) was added dropwise and the mixture became bright yellow and then precipitate formed. *N*,*N*-Dimethylpiperazine-2,3-dione (2.0 mmol, 0.284 g) was added in one portion and the flask with the suspension was placed into a water−ice bath. The mixture was stirred for 0.5 h and then aqueous NH_4Cl was added. The mixture became very dark brown-gray and then within a minute bright orange-reddish. The organic phase was separated, the aqueous phase was extracted with diethyl ether, and combined organic phases were dried over $MgSO_4$. The solvents were removed by rotary evaporation and the residue was purified by column chromatography (30 mL of silica gel, hexanes:CH_2Cl_2 (1:1) to pack the column, hexanes to elute byproduct, and then CH_2Cl_2 to elute the product). Combined fractions were subjected to rotary evaporation and product was obtained as bright orange solid (0.35 g, 32.7%). ^{1}H NMR ($CDCl_3$, 400 MHz) δ 1.51 (septet, J = 7.5 Hz, 6H), 1.17 (d, J = 7.5 Hz, 36H); $^{13}C\{^1H\}$ NMR ($CDCl_3$, 100 MHz) δ 174.0, 172.4, 149.8, 140.6, 18.4, 11.6; HRMS (EI) calcd for $C_{26}H_{42}N_2O_2S_2Si_2$ 534.2226, found 534.2241. Anal. Calcd for $C_{26}H_{42}N_2O_2S_2Si_2$: C, 58.38; H, 7.91; N, 5.24. Found: C, 58.51; H, 7.98; N, 5.16.

2,7-Bis(trimethylsilyl)benzo[2,1-*b*:3,4-*b*′]diselenophene-4,5-dione (3d). 5,5′-Bis(trimethylsilyl)-3,3′-dibromo-2,2′-diselenophene (**1d**) (1.2 mmol, 0.675 g) was dissolved in anhydrous THF (80 mL) under nitrogen atmosphere and the resulting yellow solution was cooled in an acetone/dry ice bath. *n*-Butyllithium (1.6 M in hexanes, 2.4 mmol, 1.5 mL) was added dropwise and the yellow mixture became red-orange. After the mixture was stirred for 10 min diethyl oxalate (1.1 equiv, 0.192 g) was added to a red-brown mixture and it became red. The mixture was allowed to warm to ∼0 °C and an aqueous solution of NH_4Cl was added. A very small amount of product was detected by TLC. The reddish-orange organic phase was removed and dried over $MgSO_4$ and the solvents were removed by rotary evaporation to give crude product as a reddish residue. This crude product was purified by column chromatography (30 mL of silica gel, hexanes: CH_2Cl_2 (4:1)). The solvents were removed from the combined fractions and product was obtained as a dark-red solid (∼10−15 mg, ∼3% yield). ^{1}H NMR ($CDCl_3$, 400 MHz) δ 7.92 (s with two satellites, 2H), 0.36 (s, 18H); $^{13}C\{^1H\}$ NMR ($CDCl_3$, 100 MHz) δ 175.2, 156.7, 151.1, 137.8, 136.3, −0.02; HRMS (EI) calcd for $C_{16}H_{20}O_2Se_2Si_2$ 459.9332, found 459.9356. Elemental analysis was not obtained due to the very limited amount of material.

■ ASSOCIATED CONTENT

Ⓢ Supporting Information. Cyclic voltammograms of compounds **2a**−**d** and **3a**−**d** with current units shown, copies of ^{1}H and ^{13}C NMR analyses of **2a**−**d** and **3a**−**d**, ORTEP and packing drawings for **3a** and **3c**, X-ray crystallographic files in CIF format for **2c**, **3a**, and **3c**, electronic band structure of **3c**, and tables of atom coordinates and absolute energies of **2a**−**d** and **3a**−**d** (Tables S2−S10). This material is available free of charge via the Internet at http://pubs.acs.org.

■ AUTHOR INFORMATION

Corresponding Author

*E-mail: yulia.getmanenko@chemistry.gatech.edu;seth.marder@chemistry.gatech.edu.

■ ACKNOWLEDGMENT

This material is based upon work supported in part by Solvay S.A., by the STC Program of the National Science Foundation under Agreement No. DMR-0120967, and by the PREM Program of the NSF under Agreement No. DMR-0934212.

■ REFERENCES

(1) Bao, Z. A.; Lovinger, A. J.; Brown, J. *J. Am. Chem. Soc.* **1998**, *120*, 207–208.
(2) Katz, H. E.; Johnson, J.; Lovinger, A. J.; Li, W. J. *J. Am. Chem. Soc.* **2000**, *122*, 7787–7792.
(3) Jones, B. A.; Facchetti, A.; Marks, T. J.; Wasielewski, M. R. *Chem. Mater.* **2007**, *19*, 2703–2705.
(4) Handa, S.; Miyazaki, E.; Takimiya, K.; Kunugi, Y. *J. Am. Chem. Soc.* **2007**, *129*, 11684–11685.
(5) Usta, H.; Risko, C.; Wang, Z. M.; Huang, H.; Deliomeroglu, M. K.; Zhukhovitskiy, A.; Facchetti, A.; Marks, T. J. *J. Am. Chem. Soc.* **2009**, *131*, 5586–5608.
(6) Yoon, M. H.; DiBenedetto, S. A.; Facchetti, A.; Marks, T. J. *J. Am. Chem. Soc.* **2005**, *127*, 1348–1349.
(7) Yoon, M. H.; DiBenedetto, S. A.; Russell, M. T.; Facchetti, A.; Marks, T. J. *Chem. Mater.* **2007**, *19*, 4864–4881.
(8) Ie, Y.; Nitani, M.; Karakawa, M.; Tada, H.; Aso, Y. *Adv. Funct. Mater.* **2010**, *20*, 907–913.
(9) Ohnishi, H.; Kozaki, M.; Okada, K. *Synth. Met.* **2003**, *135*, 85–86.
(10) Letizia, J. A.; Cronin, S.; Ortiz, R. P.; Facchetti, A.; Ratner, M. A.; Marks, T. J. *Chem.—Eur. J.* **2010**, *16*, 1911–1928.
(11) Brzezinski, J. Z.; Reynolds, J. R. *Synthesis* **2002**, 1053–1056.
(12) Lambert, T. L.; Ferraris, J. P. *Chem. Commun.* **1991**, 752–754.
(13) Ferraris, J. P.; Lambert, T. L. *Chem. Commun.* **1991**, 1268–1270.
(14) Mills, C. A.; Taylor, D. M.; Murphy, P. J.; Dalton, C.; Jones, G. W.; Hall, L. M.; Hughes, A. V. *Synth. Met.* **1999**, *102*, 1000–1001.
(15) Takahashi, K.; Fujita, S.; Akiyama, K.; Miki, M.; Yanagi, K. *Angew. Chem., Int. Ed.* **1998**, *37*, 2484–2487.
(16) Kozaki, M.; Yonezawa, Y.; Okada, K. *Org. Lett.* **2002**, *4*, 4535–4538.
(17) Kozaki, M.; Yonezawa, Y.; Igarashi, H.; Okada, K. *Synth. Met.* **2003**, *135*, 107–108.
(18) Ie, Y.; Nitani, M.; Ishikawa, M.; Nakayama, K.; Tada, H.; Kaneda, T.; Aso, Y. *Org. Lett.* **2007**, *9*, 2115–2118.
(19) Loganathan, K.; Cammisa, E. G.; Myron, B. D.; Pickup, P. G. *Chem. Mater.* **2003**, *15*, 1918–1923.
(20) Coppo, P.; Cupertino, D. C.; Yeates, S. G.; Turner, M. L. *J. Mater. Chem.* **2002**, *12*, 2597–2599.
(21) Tarutani, S.; Takahashi, K. *Bull. Chem. Soc. Jpn.* **2004**, *77*, 463–475.
(22) Wynberg, H.; Sinnige, H. J. M. *Recl. Trav. Chim. Pays-Bas* **1969**, *88*, 1244–1245.
(23) Guegano, X.; Kanibolotsky, A. L.; Blum, C.; Mertens, S. F. L.; Liu, S. X.; Neels, A.; Hagemann, H.; Skabara, P. J.; Leutwyler, S.; Wandlowski, T.; Hauser, A.; Decurtins, S. *Chem.—Eur. J.* **2009**, *15*, 63–66.
(24) Mondal, R.; Becerril, H. A.; Verploegen, E.; Kim, D.; Norton, J. E.; Ko, S.; Miyaki, N.; Lee, S.; Toney, M. F.; Bredas, J.-L.; McGehee, M. D.; Bao, Z. N. *J. Mater. Chem.* **2010**, *20*, 5823–5834.
(25) Getmanenko, Y. A.; Tongwa, P.; Timofeeva, T. V.; Marder, S. R. *Org. Lett.* **2010**, *12*, 2136–2139.

(26) Preparation of **2a** (88.5% yield by NMR) using dimethylcarbamoyl chloride was independently reported in the following patent: Kirner, H. J.; Bienewald, F.; Flores, J.-C.; Aebischer, O. F. International Publication No. WO 2009/115413 A2, 2009.
(27) Barlow, S.; Odom, S. A.; Lancaster, K.; Getmanenko, Y. A.; Mason, R.; Coropceanu, V.; Bredas, J.-L.; Marder, S. R. *J. Phys. Chem. B* **2010**, *114*, 14397–14407.
(28) Lower (in comparison with non-alkylated version) yields for a similarly structured material, 2,6-bis(3,5-bis(*n*-dodecyl)trimethylsilyl)cyclopenta[2,1-*b*;3,4-*b*′]dithiophen-4-one (58% crude yield), were reported in the following patent: Kirner, H. J.; Bienewald, F.; Flores, J.-C.; Aebischer, O. F. International Publication No. WO 2009/115413 A2, 2009.
(29) Muellerwesterhoff, U. T.; Ming, Z. *Tetrahedron Lett.* **1993**, *34*, 571–574.
(30) Muellerwesterhoff, U. T.; Zhou, M. *J. Org. Chem.* **1994**, *59*, 4988–4992.
(31) A 46% yield for **3a** using *N*,*N*-dimethylpiperazine-2,3-dione and a 40% yield of 2,7-bis(trimethylsilyl)-3,6-di-*n*-dodecylbenzo[2,1-*b*:3,4-*b*′]dithiophene-4,5-dione were reported in the following patent: Kirner, H. J.; Bienewald, F.; Flores, J.-C.; Aebischer, O. F. International Publication No. WO 2009/115413 A2, 2009.
(32) Wang, Y. K.; Shu, C. F.; Breitung, E. M.; McMahon, R. J. *J. Mater. Chem.* **1999**, *9*, 1449–1452.
(33) Koopmans, T. *Physica* **1934**, *1*, 104–113.
(34) Connelly, N. G.; Geiger, W. E. *Chem. Rev.* **1996**, *96*, 877–910.
(35) Kozaki, M.; Tanaka, S.; Yamashita, Y. *J. Org. Chem.* **1994**, *59*, 442–450.
(36) Howie, R. A.; Wardell, J. L. *Acta Crystallogr., Sect. E: Struct. Rep. Online* **2006**, *62*, O659–O661.
(37) Mas-Torrent, M.; Hadley, P.; Bromley, S. T.; Ribas, X.; Tarres, J.; Mas, M.; Molins, E.; Veciana, J.; Rovira, C. *J. Am. Chem. Soc.* **2004**, *126*, 8546–8553.
(38) Valeev, E. F.; Coropceanu, V.; da Silva, D. A.; Salman, S.; Bredas, J.-L. *J. Am. Chem. Soc.* **2006**, *128*, 9882–9886.
(39) Becke, A. D. *Phys. Rev. A: At., Mol., Opt. Phys.* **1988**, *38*, 3098–3100.
(40) Becke, A. D. *J. Chem. Phys.* **1993**, *98*, 5648–5652.
(41) Lee, C.; Yang, W.; Parr, R. G. *Phys. Rev. B: Condens. Matter Mater. Phys.* **1988**, *37*, 785.
(42) Frisch, M. J. T., G. W.; Schlegel, H. B.; Scuseria, G. E.; Robb, M. A.; Cheeseman, J. R.; Scalmani, G.; Barone, V.; Mennucci, B.; Petersson, G. A.; Nakatsuji, H.; Caricato, M.; Li, X.; Hratchian, H. P.; Izmaylov, A. F.; Bloino, J.; Zheng, G.; Sonnenberg, J. L.; Hada, M.; Ehara, M.; Toyota, K.; Fukuda, R.; Hasegawa, J.; Ishida, M.; Nakajima, T.; Honda, Y.; Kitao, O.; Nakai, H.; Vreven, T.; Montgomery, J. A., Jr.; Peralta, J. E.; Ogliaro, F.; Bearpark, M.; Heyd, J. J.; Brothers, E.; Kudin, K. N.; Staroverov, V. N.; Kobayashi, R.; Normand, J.; Raghavachari, K.; Rendell, A.; Burant, J. C.; Iyengar, S. S.; Tomasi, J.; Cossi, M.; Rega, N.; Millam, N. J.; Klene, M.; Knox, J. E.; Cross, J. B.; Bakken, V.; Adamo, C.; Jaramillo, J.; Gomperts, R.; Stratmann, R. E.; Yazyev, O.; Austin, A. J.; Cammi, R.; Pomelli, C.; Ochterski, J. W.; Martin, R. L.; Morokuma, K.; Zakrzewski, V. G.; Voth, G. A.; Salvador, P.; Dannenberg, J. J.; Dapprich, S.; Daniels, A. D.; Farkas, Ö.; Foresman, J. B.; Ortiz, J. V.; Cioslowski, J.; Fox, D. J. *Gaussian 09*; Gaussian Inc., Wallingford, CT, 2009.
(43) Thompson, M. A. *ArgusLab 4.0.1*; Planaria Software, LLC, Seattle, WA.
(44) Kresse, G.; Furthmuller, J. *Phys. Rev. B* **1996**, *54*, 11169–11186.
(45) Kresse, G.; Furthmuller, J. *Comput. Mater. Sci.* **1996**, *6*, 15–50.
(46) Wang, Y.; Perdew, J. P. *Phys. Rev. B* **1991**, *43*, 8911–8916.
(47) Sheldrick, G. M. *SADABS*, V.2.0.3, Bruker/Siemens area detector absorption correction program; Bruker AXS, Madison, WI, 2003.
(48) Sheldrick, G. M. *TWINABS*; Bruker AXS, Madison, WI, 2002.
(49) *SAINTP+* for *NT*, v.6.2, *data reduction and correction program*; Bruker AXS: Madison, WI, 2001.
(50) Sheldrick, G. M. *SHELXTL NT*, v. 6.12, structure determination software suite; Bruker AXS, Madison, WI, 2001.
(51) Stangeland, E. L.; Sammakia, T. *J. Org. Chem.* **2004**, *69*, 2381–2385.